International Research Journal of Engineering and Technology (IRJET) e-ISSN: 2395-0056
Volume: 09 Issue: 04 | Apr 2022 www.irjet.net p-ISSN: 2395-0072

Monitoring NDTI-River Temperature relationship along the river ganga in the segments around Ghazipur, Varanasi & Mirzapur district using Geo-spatial techniques

Vandana Gupta[1], Rajarshi Bhattacharjee[2], Dr. Shishir Gaur[3] , Shri Arjun Singh[4]

[1]M.Tech in RS & GIS , RSAC-UP, Lucknow, Uttar Pradesh, India
[2]Junior Research Fellow, Department of Civil Engineering, IIT BHU, Varanasi, India
[3]Assistant Professor, Department of Civil Engieering, IIT BHU, Varanasi, India
[4]Scientist-SD, RSAC-UP, Lucknow, Uttar Pradesh, India

Abstract – *The present study monitors the interrelationship of Quantative analysis has been performed for river temperature and Normalised Difference Turbidity Index (NDTI) respectively for river water quality assessment. Ghazipur, Varanasi, and Mirzapur stretches have been selected for this study. The temporal variation in turbidity and temperature was analyzed for the years 2010, 2015, 2019 & 2021 using LANDSAT-5,8 archive. In this study, it has been found that the Varanasi stretch showcases the highest river temperature followed by Mirzapur and Ghazipur stretches respectively. The river turbidity derived through NDTI also follows the same pattern. This can be attributed to impact of high population contributing to domestic and industrial waste flowing into river Ganga in vicinity to Varanasi city. Statistical analysis highlights the high correlation coefficient and regression coefficient values i.e., 0.834 & 0.696 respectively between turbidity and temperature along Varanasi stretch followed by correlation coefficient and regression coefficient values of 0.809 & 0.655 along Mirzapur stretch and values of 0.809 & 0.654 for river stretch along Ghazipur for the corresponding years. The study elicites the impact of turbidity on river temperature and also emphasizes the use of Geospatial technique to make quantitative estimates, even in the absence of field observations.*

Key Words: **LANDSAT; Turbidity; NDTI; river temperature.**

1. INTRODUCTION

The mapping of the river or the inland water quality using remote sensing technology was not new for the scientific community, and this activity has been practiced since the 1970s with the launch of the Landsat series of satellites (Klemas *et al.* 1971; Ritchie *et al.*1976). The conventional procedures for testing the water quality parameters are expensive as well as time-consuming, and it provides information only for the point(s) under measurement. The remote sensing technology can be utilized as an advantageous alternative option in this regard (Novo *et al.* 2006; Lamaro *et al. 2013*). Every earth's surface features behave uniquely while interacting with electromagnetic radiation (EMR). This distinctiveness generates in the form of the spectral signature from each surface feature, and this signature has been utilized to identify the surface feature through satellite images. When a slight change in the composition of a feature occurs, it simultaneously changes the spectral signature(Moore 1980). Several factors accompany the change of the spectral signature for a feature, and the same can be valid for the water feature. Some of the factors responsible for generating the different spectral signatures of water are the elevation angle of the sun, the season of the year, water surface roughness, turbidity, depth of the water, and vegetation growth on the water surface (Garg *et al.* 2020). By studying these different spectral signatures, and sometimes the quantitative assessment of a particular component can be accomplished (Chander *et al.* 2019; Luis *et al.* 2019) with the help of remote sensing technology.

The river temperature is one of the crucial parameters as it influences the river ecology and marine life (Caissie, 2006; Ling et al., 2017; Smith, 2008; Wawrzyniak et al., 2012). The temperature of the water is one of the significant parameters because it is helpful in regulating the rate of chemical reactions in the river. The continuum concept of the river signifies that any change in the river temperature can intensely impact the longitudinal distribution of organisms in the fluvial ecosystem (Vannote *et al.* 1980; Wawrzyniak et al., 2012). Biological processes of the aquatic species, such as growth, reproduction, and survival rate, show a decreasing trend when stream temperature in the river rises above a specific threshold value (Eaton et al. 1995; Xin and Kinouchi, 2013). According to Vant's Hoff theory, it can be stated that for every 10ºC rise in the temperature of the water, the biological activity nearly doubles within the temperature range of 0-40°C under normal situations (Gillooly *et al.* 2001; Caissie 2006). In comparison to the in-situ measurements, the remote sensing techniques provide alluring possibilities for estimating and observing the river temperature as well the spatial thermal pattern of the river (Ling *et al.* 2017). Several researchers are now using remote sensing technology for estimating the river temperature. The thermal bands present in the LANDSAT satellite system have been used for this purpose (Lamaro *et al.* 2013; Wawrzyniak *et al.* 2016).

Turbidity is another essential water quality parameter where suspended sediments, instead of transmitting the light along the water column it scatters the light (Sebastiá-Frasquet *et al.* 2019). When the concentration of suspended solids or sediments in water increases, the turbidity also gets enhanced (Ritchie *et al.* 1976; Garg *et al.* 2017). The higher value of turbidity escalates the opacity of the water, which in turn hampers aquatic life (Quang *et al.* 2017; Sebastiá-Frasquet *et al.* 2019). Several researchers have mentioned that temporal change in the concentration of the river turbidity can occur because of the variation in the weather and climate pattern and also due to the human activities near the bank of the river (Luis *et al.* 2019; Garg *et al.* 2020).

In this present work, an attempt has been made for analysing the water quality parameters like temperature & turbidity for the river Ganga at Ghazipur, Varanasi, and Mirzapur stretches. The temporal study of the Landsat-8 and Ladsat-5 data have been performed for the year 2010, 2015, 2019 and 2021 .

Cloud-free satellite images have been considered for this study.For the processing of the image ArcGIS Desktop platform has been used. Satellite images freely available from USGS Earth Explorer, no field data was collected for this time period, the results are calculated by existing algorithms for calculating the temperature of the river temperature and NDTI used in this analysis.

2.MATERIALS AND METHODS

2.1. Study area

The selected stretch area lies between Ghazipur and Mirzapur is located in the northern part of India in south-eastern Uttar Pradesh between the coordinates 82.56°E, 25.13°N to 83.57°E, 25.58°N (Yadav *et al.* 2020). This segment of the river comes under the geomorphological unit of Central Ganga Plains. In this region, the Ganga river plain is flat alluvial in nature, having a shallow depression and a small eastward gradient. The width of the river varies between 700-750 meters in the study stretch, and the average height of this region is 76.19 meters above the mean sea level (Rai *et al.* 2010; Pandey and Singh, 2017). In this part, the summer season usually has a longer duration as compared to the winter season. The summer temperature varies between 32- 47°C, whereas the winter temperature hovers around the range of 5-15°C mostly. Varanasi is a very famous city which lies in this region, and it is also called the spiritual capital of India. This city is also famous for silk products, ivory, and sculptures (Garg *et al.* 2020). This work has been performed on the river stretch situated near the three cities that lies in the study area. The three stretches have been marked with red colour for which the work has been performed. The location map has been drawn in Figure1.

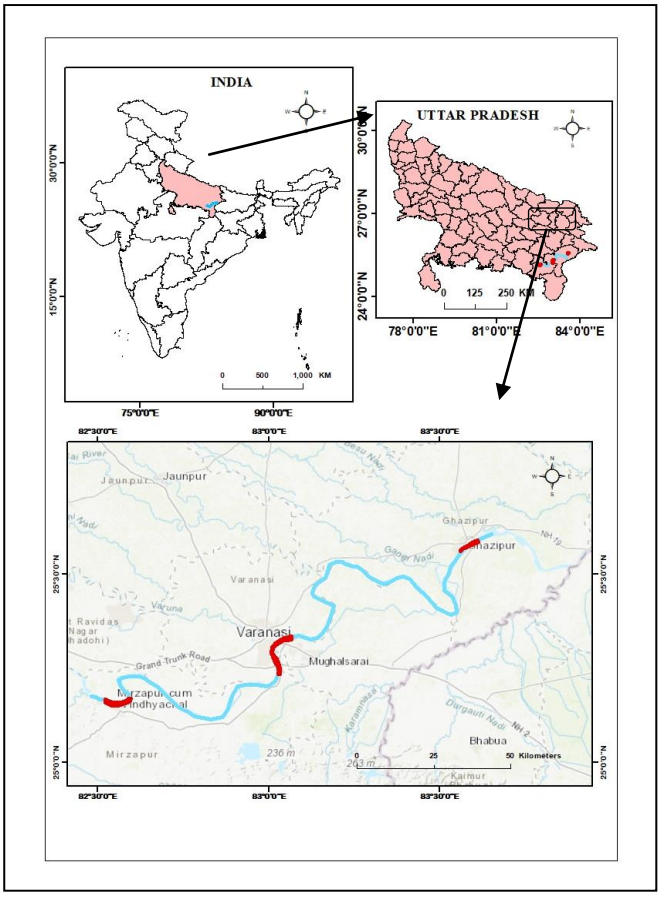

Fig. 1. Location map of study area.

2.2. Satellite imagery datasets

The essential information source for this work was a series of Landsat-8 and Landsat-5 satellite images. Landsat-8 satellite consist of 11 bands of different wavelengths among which there are two thermal infrared (TIR) bands namely, band 10 (10.60-11.9µm) and band 11 (11.50-12.51µm). And Landsat-5 satellite consist of 8 bands of different wavelengths among which there is one thermal infrared (TIR) bands namely, band 6 (10.40-12.50µm) . The Landsat scenes were selected for this study having path id "142" and row id "42" and "43". The chosen Landsat scenes were for the years 2010,2015,2019 and 2021, having almost 0% cloud cover and were freely downloaded from the United States Geological Survey Earth Explorer site. All the images were Level 1T products, which have been precision and terrain corrected in Geo-TIFF format and are in the UTM Zone 44N projection and WGS-84 as ellipsoidal datum (http://earthexplorer.usgs.gov) (Ling et al., 2017; Reuter et al., 2015). The details of stretch wise satellite data used are given in Table 1.

CITY	SENSOR	DATE	PATH/ROW
VARANASI	Landsat-8	05/04/2021	142/42
	Landsat-8	18/05/2019	142/42
	Landsat-8	23/05/2015	142/42
	Landsat-5	25/05/2010	142/42
MIRZAPUR	Landsat-8	05/04/2021	142/43
	Landsat-8	03/06/2019	142/43
	Landsat-8	23/05/2015	142/43
	Landsat-5	25/05/2010	142/43
GHAZIPUR	Landsat-8	05/04/2021	142/42
	Landsat-8	18/05/2019	142/42
	Landsat-8	23/05/2015	142/42
	Landsat-5	25/05/2010	142/42

Table -1: The list of satellite data used in the study.

2.3.Methodology adopted for this analysis

Flowchart for the spatio-temporal analysis of the water quality parameters have been drawn in **figure 2**.

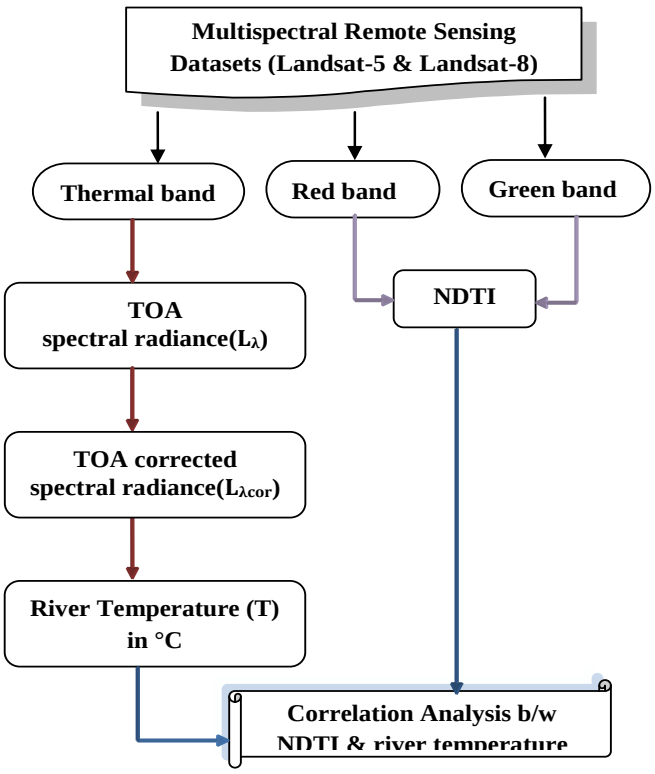

Fig. 2. Flowchart of the methodology

2.3.a. Estimation of turbidity through NDTI

It has also been reported in the literature that relying on a single band or algorithm sometimes results in overestimation or underestimation of suspended sediment concentration (Kuhn et al. 2019; Pahlevan et al. 2019). It was suggested, either use combination of sensitive bands or different algorithms to reach the final conclusion. Therefore, an attempt has been made to qualitatively estimate the temporal turbidity in each stretch using the NDTI developed by Lacaux et al. (2007).

$$NDTI = (R_R - R_G) / (R_R + R_G) \quad (1)$$

Where R_R and R_G is the reflectance in the red and green band. Generally, the reflectance of pure water is more in green than the red wavelength region. However, it has been reported that the red region reflectance increases with an increase in turbidity. Therefore, the red and green bands were used to enhance the image for turbidity. Initially, the water pixels were identified as mentioned above, then Eq. was applied using these two bands to map NDTI. The higher value of turbidity yields a high value of NDTI and vice versa.

2.3.b. Estimation of river temperature

The atmospheric correction of the radiance of thermal band involves the elimination of atmospheric effects, which imparts noise in the signal received by the sensors. For the corrected water surface radiance, several atmospheric parameters like $L_{\lambda up}$(upwelling radiance), τ(atmospheric transmissivity), $L_{\lambda d}$(downwelling radiance) will be required and in addition to these parameters 'ε' (water emissivity) value will also be needed. Atmospheric parameters ($L_{\lambda up}$, τ, $L_{\lambda d}$) were obtained from 'Atmosphere Correction Parameter Calculator'(http://www.atmcorr.gsfc.nasa.gov/) (Lamro et al. 2013; Ling et al., 2017). In this work, emissivity of water was taken as 0.9885 (Simon et al., 2014).

For river temperature estimation, we have to calculate Top of Atmosphere (TOA) spectral radiance first, using formula:

$$L_\lambda = M_L * Q_{cal} + A_L \quad (2)$$

where L_λ is the TOA spectral radiance (Watts/(m^2*srad*μm)), M_L is Band-Specific Multiplicative re-scaling factor from metadata, Q_{cal} is quantized and calibrated standard product pixel value DN and A_L is Band-Specific additive re-scaling factor from metadata. Afterwards, calculated TOA value is corrected by using the formula:

$$L_{\lambda cor} = \tau.\varepsilon.L_\lambda + L_{\lambda up} + L_{\lambda d}(1-\varepsilon).\tau \quad (3)$$

where, symbols have the usual meanings and these meanings have been already described above. Then, the spectral radiance can be converted to brightness temperature in degree Celsius using the following formula:

$$T = [K2 / (\ln((K1 / L_{\lambda cor}) + 1))] - 273.15 \quad (4)$$

where, K1 and K2 are thermal constant of the satellite (Barsi et al., 2014; Rajeshwari and Mani, 2014). Value of M_L and A_L of the study area is 0.000342 and 0.1 respectively. The value of K1 and K2 of the satellite's band 10(Landsat-8) for study area is 774.8853 and 1321.0789. The value of K1 and K2 of the satellite's band 6(Landsat-5) for study area is 607.76 and 1260.56.These values we can get from metadata file of the satellite image (http://earthexplorer.usgs.gov) (Rajeshwari and Mani, 2014).

3. RESULTS AND DISCUSSION

3.1.Map Layout representation of river temperature and NDTI values

The result has been presented in the form of the line graph for river temperature and NDTI during the time period for the years 2010, 2015, 2019, 2021. Different months (April, May and June) have been chosen for this study because of the cloud cover issue associated with LANDSAT -8 AND LANDSAT -5 imageries.

- River temperature in the Ghazipur region during 2010 lies between 24.80°C to 28.40°C with average value of 28.44°C; during 2015 lies between 27.80°C to 36.50°C with average value of 29.39°C; during 2019 lies between 25.10°C to 34.50°C with average value of 26.71°C and for the period of 2021, the temperature situated between 23.30°C and 36.60°C with average value of 25.02°C with most of the values falls within 26.1°C.
- For the Varanasi region, the temperature range for 2010 lies between 24.90°C to 29.70°C with average value of 29.67°C; during 2015 lies between 28.10°C to 39.40°C with average value of 29.68°C; during 2019 lies between 24.60°C to 32.30°C with average value of 26.1°C and for the period of 2021, the temperature situated between 23.70°C and 35.30°C with average value of 25.73°C.
- The Mirzapur region also shows a similar trend to that of Varanasi and Ghazipur. The significant temperature range of 2010 lies between 27.80°C to 31.30°C with average value of 28.54°C; during 2015 lies between 28.40°C to 36.20°C with average value of 29.86°C; during 2019 lies between 25.40°C to 27.85°C with average value of 26.45°C and for the period of 2021, the temperature situated between 24.70°C and 32.40°C with average value of 25.87°C .

The NDTI values have been calculated for the time period of 2010, 2015, 2019, and 2021 using LANDSAT datasets. The NDTI trend for all three stretches shows a similar pattern shows a slight downward trend.

- For the period of 2010, the NDTI range of Ghazipur, Varanasi, and Mirzapur are -0.01 to 0.03, -0.03 to 0.02, and -0.03 to 0.02, respectively with the average values of -0.01, -0.02, -0.02.
- For the period of 2015, the NDTI range of Ghazipur, Varanasi, and Mirzapur are -0.04 to 0.04, -0.05 to 0.04, and -0.04 to 0.03, respectively with the average values of -0.02, -0.03, -0.03.
- For the period of 2019, the NDTI range of Ghazipur, Varanasi, and Mirzapur are -0.04 to 0.03, -0.04 to 0.03, and -0.05 to 0.03, respectively with the average values of -0.02, -0.03, -0.03.
- For the period of 2021, the NDTI range of Ghazipur, Varanasi, and Mirzapur are -0.04 to 0.03, -0.05 to 0.04, and -0.05 to 0.03, respectively with the average values of -0.03, -0.04, -0.04.

Figure-3,4,&5 shows map yayout Representation for NDTI & River Temperature for the three stretches. And Figure-3(a),(b); 4(a),(b) & 5(a),(b) shows line graph representation for (a) Avg.NDTI (b)Avg.River Temperature(°C) for the three stretches.

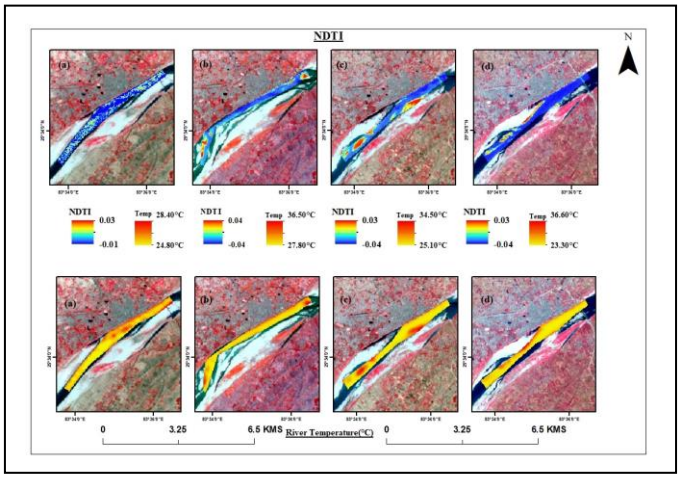

Fig. 3. Map Layout Representation for NDTI & River Temperature for Ghazipur stretch.

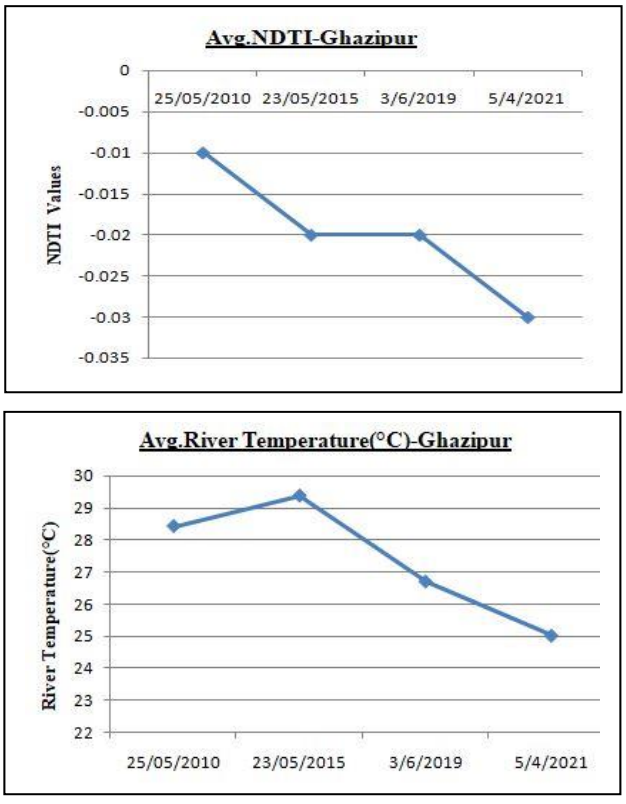

Fig. 3: Line Graph Representation for (a)Avg.NDTI (b)Avg.River Temperature(°C) for Ghazipur stretch.

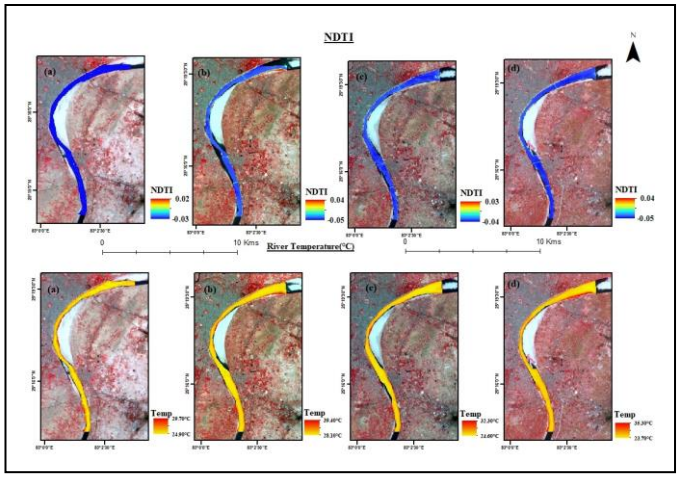

Fig. 4. Map Layout Representation for NDTI & River Temperature for Varanasi stretch.

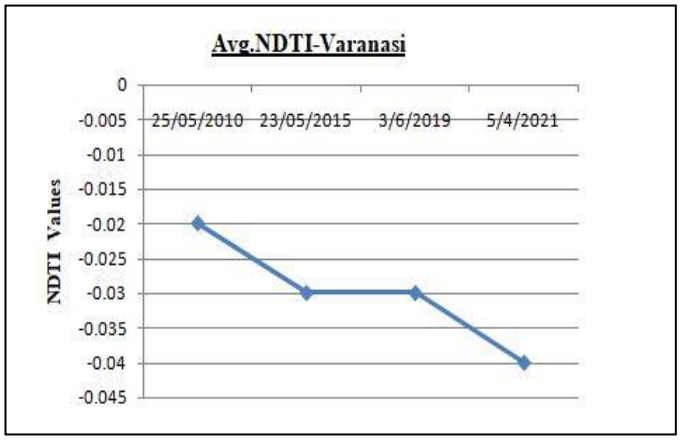

Fig. 4(a): Line Graph Representation for Avg.NDTI for Varanasi stretch.

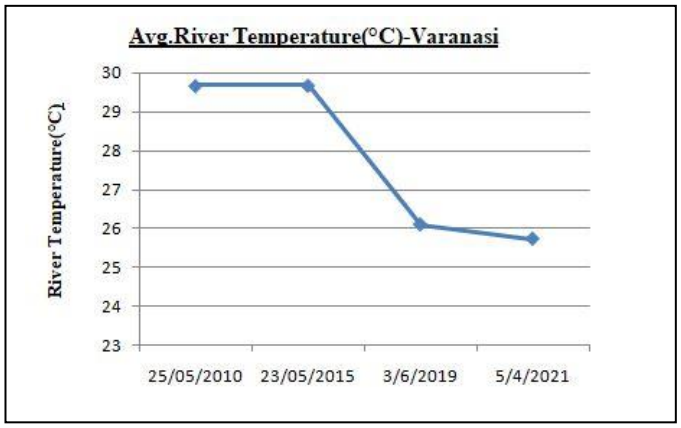

Fig. 4(b): Line Graph Representation for Avg.River Temperature(°C) for Varanasi stretch.

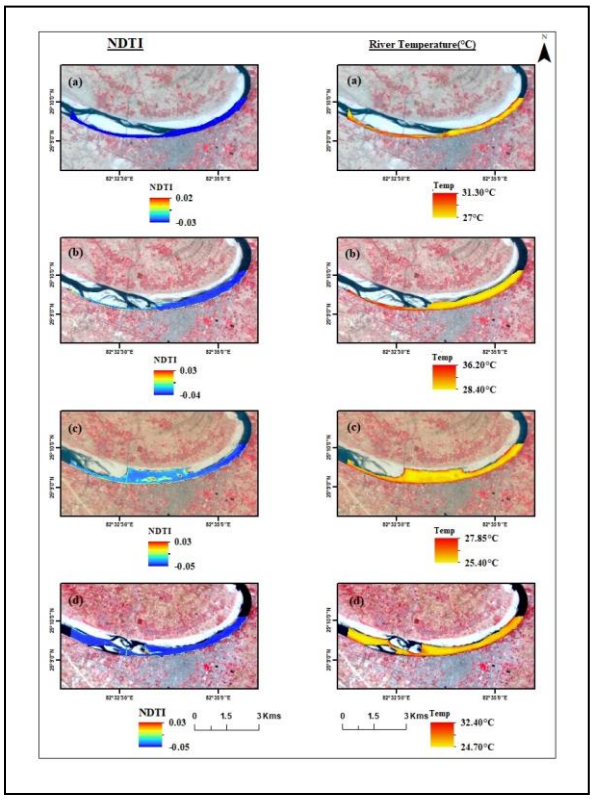

Fig. 5. Map Layout Representation for NDTI & River Temperature for Mirzapur stretch.

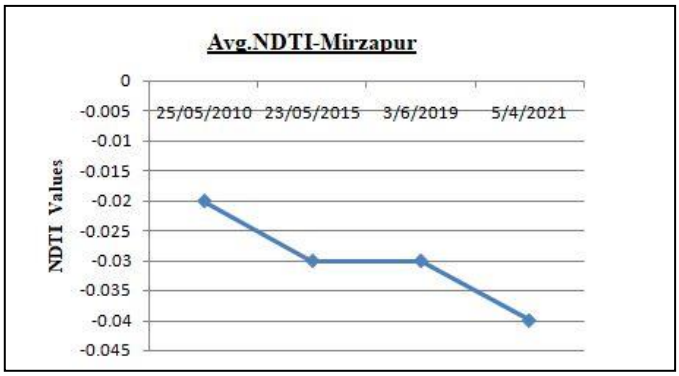

Fig. 5(a) Line Graph Representation for Avg.NDTI for Mirzapur stretch.

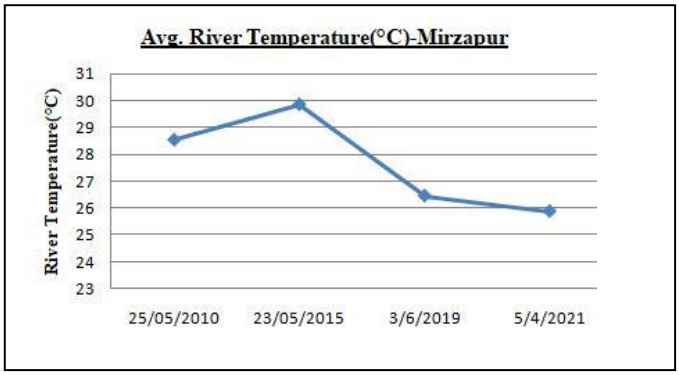

Fig. 5(b): Line Graph Representation for Avg.River Temperature(°C) for Mirzapur stretch.

3.2 Relation between river temperature and NDTI

The correlation graphs have been plotted for the Ghazipur, Varanasi and Mirzapur region. NDTI values has been plotted on X-axis and river temperature has been plotted on Y-axis.

By calculating the correlation between River temperature and NDTI, it can be clearly noticed that both the parameters are directly propotional to each other.

When the temperature is greater, the NDTI value is also greater which points out the increase in the turbidity values.They show a high positive correlation.

The correlation between river temperature and NDTI is 0.655 for Varanasi stretch, 0.696 for Mirzapur Stretch and 0.654 for Ghazipur stretch. Fig.6(a), Fig.6(b). and Fig.6(c) shows the correlation graph b/w river temperature and NDTI for Ghazipur, Varanasi and Mirzapur stretch.

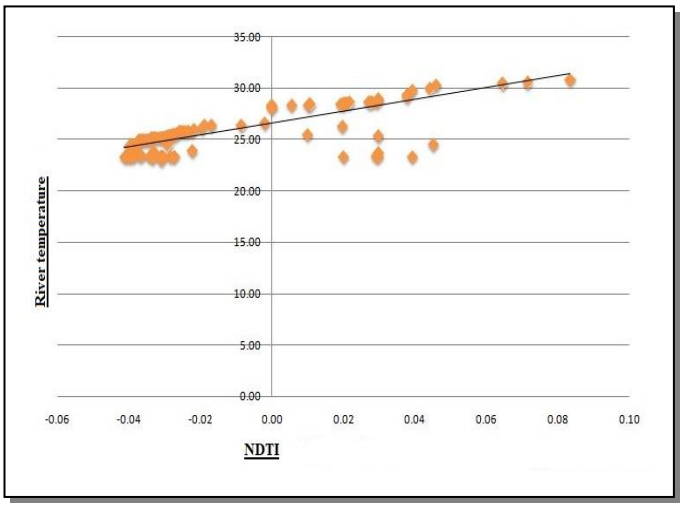

Fig. 6(a): Correlation graph b/w river temperature and NDTI for Ghazipur stretch

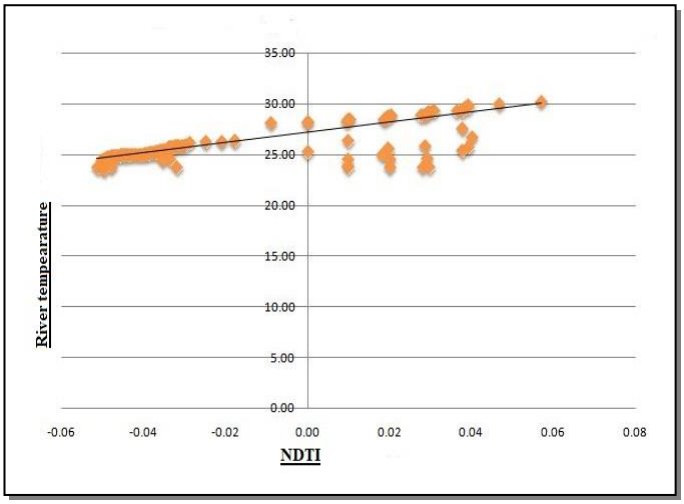

Fig. 6(b): Correlation graph b/w river temperature and NDTI for Varanasi stretch.

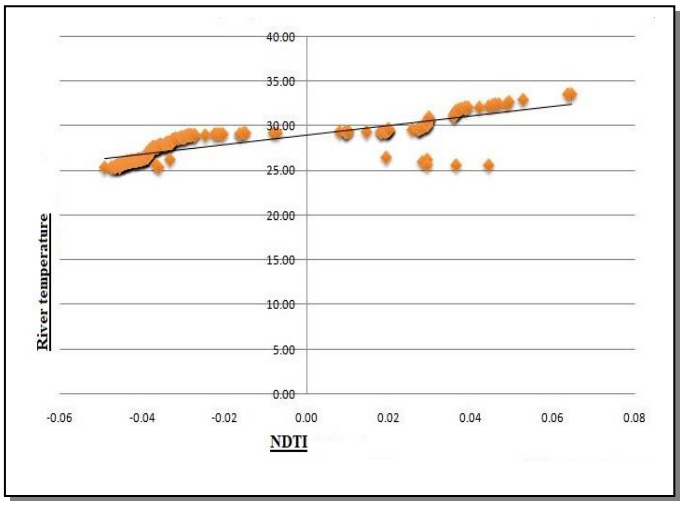

Fig. 6(c): Correlation graph b/w river temperature and NDTI for Mirzapur stretch.

3.3. Special emphasis for the Varanasi stretch

Varanasi city is one of the most populated cities in the country and also one of the very famous places of Vedic culture. It is the most populated and important city of the considered river stretch.This is the region worst affected by polluted water of the river as the huge number of the population in this region depends on the river water for their numerous works. The aquatic ecosystem in this region has been hampered heavily due to anthropogenic and industrial activities. Moreover, in this stretch, two rivers Varuna and Assi, have joined with the river Ganga and these rivers bring immense waste along with them. If the river restoration work can be adequately performed in this region, then for the other areas of the considered stretch, it would not be a very challenging task.

5. CONCLUSIONS

Satellite imageries have been used for the spatio-temporal analysis of the river water quality parameter in the considered study stretch for the years 2010 ,2015, 2019 and 2021.

- In the Mirzapur stretch, the temperature of the river Ganga decreases most in 2019 by 3.41°C as compared to 2015 then in 2021 decreases by 0.58°C as compared to 2019.
- Similarly, in the Varanasi stretch, the temperature had been reduced most in 2019 by 3.58°C as compared to 2015 then in 2021 decreases by 0.37°C as compared to 2019
- And in the Ghazipur stretch, this decline of the temperature of the river was noted as 2.68°C in 2019 as compared to 2015 then in 2021 decreases by 1.69°C as compared to 2019.

The decrease in the NDTI value showed a different trend.

- In the Mirzapur stretch, the NDTI of the river Ganga decreases by 0.01 in 2015 as compared to 2010 , then in 2019 shows similar trend as compared to 2015 then in 2021 also decreases by 0.01 as compared to 2019.
- Similarly, in the Varanasi and Ghazipur stretch shows similar trend as Mirzapur stretch.

ACKNOWLEDGEMENT

The author deeply thanks to co-authors to carry forward this study and for the technical and theoretical support and continuous support in writing part of this research paper.

REFERENCES

[1] Klemas V, Borchardt J F and Treasure W M; "Suspended sediment observations from ERTS-1", Remote Sensing of Environment, 2, 205-221, (1971).

[2] Ritchie J, Schiebe F R and McHenry J R; "Remote sensing of suspended sediments in surface waters", Photogrammetric Engineering & Remote Sensing, 42(12), 1539–1545, (1976).

[3] de Moraes Novo E M L, de Farias Barbosa C C, de Freitas R M, Shimabukuro Y E, Melack J M and Pereira Filho W; "Seasonal changes in chlorophyll distributions in Amazon floodplain lakes derived from MODIS images"; Limnology 7:153–161,(2006).

[4] Lamaro A A, Mariñelarena A, Torrusio S E and Sala S E; "Water surface temperature estimation from Landsat 7 ETM+ thermal infrared data using the generalized single-channel method: Case study of Embalse del Río Tercero (Córdoba, Argentina)"; Advances in Space Research, 51(3), 492-500, (2013).

[5] Moore G K; "Satellite remote sensing of water turbidity", Hydrological Science Journal, 25(4), 407-421, (1980).

[6] Garg V, Aggarwal S P and Chauhan P; "Changes in turbidity along Ganga River using Sentinel-2 satellite data during lockdown associated with COVID-19", Geomatics, Natural Hazards and Risk, 11(1), 1175-1195, (2020).

[7] Chander S, Gujrati A, Hakeem K A, Garg V, Issac A M, Dhote P R; "Water quality assessment of River Ganga and Chilika lagoon using AVIRIS-NG hyperspectral data", Current Science , 116(7), 1172-1181, (2019).

[8] Luis K M, Rheuban J E, Kavanaugh M T, Glover D M, Wei J, Lee Z and Doney S C; "Capturing coastal water clarity variability with Landsat 8", Marine Pollution Bulletin, 145, 96-104, (2019).

[9] Caissie D; "The thermal regime of rivers: a review"; Freshwater biology, 51(8), 1389-1406, (2006).

[10] Ling F, Foody G M, Du H, Ban X, Li X, Zhang Y and Du Y; "Monitoring thermal pollution in rivers downstream of dams with Landsat ETM+ thermal infrared images"; Remote Sensing , 9(11), 1175, (2017).

[11] K. Smith, "River water temperatures: an environmental review". Scottish Geographical Magazine.88, 211–220, (2008).

[12] Wawrzyniak V, Piégay H and Poirel A; "Longitudinal and temporal thermal patterns of the French Rhône River using Landsat ETM+ thermal infrared images"; Aquatic sciences, 74, 405–414, (2012).

[13] Vannote R L, Minshall G W, Cummins K W, Sedell J R and Cushing C E, "The river continuum concept"; Canadian Journal of Fisheries and Aquatic Sciences, 37(1), 130-137, (1980).

[14] Eaton J G, McCormick J H, Goodno B E, O'brien D G, Stefany H G, Hondzo M and Scheller R M, "A field information-based system for estimating fish temperature tolerance"; Fisheries 20(4), Pages 10-18, (1995).

[15] Xin Z and Kinouchi T; "Analysis of stream temperature and heat budget in an urban river under strong anthropogenic influences"; Journal of Hydrology, 489, 16-25, (2013).

[16] Gillooly J F, Brown J H, West G B, Savage V M and Charnov E L; "Effects of size and temperature on metabolic rate"; Science, 293(5538), 2248-2251, (2001).

[17] Wawrzyniak V, Piégay H, Allemand P, Vaudor L, Goma R and Grandjean P; "Effects of geomorphology and groundwater level on the spatio-temporal variability of riverine cold water patches assessed using thermal infrared (TIR) remote sensing"; Remote Sensing of Environment, 175, 337-348, (2016).

[18] Sebastiá-Frasquet M T, Aguilar-Maldonado J A, Santamaría-Del-Ángel E and Estornell J ; "Sentinel 2 analysis of turbidity patterns in a coastal lagoon"; Remote Sensing, 11(24), 2926, (2019).

[19] Garg V, Kumar A S, Aggarwal S P, Kumar V, Dhote P R, Thakur P K, "Spectral similarity approach for

mapping turbidity of an inland waterbody"; Journal of Hydroogy, **550,** 527-537, (2017).

[20] Quang N H, Sasaki J, Higa H and Huan N H, "Spatiotemporal variation of turbidity based on landsat 8 oli in cam ranh bay and thuy trieu lagoon, Vietnam"; Water, **9(8),** 570, (2017).

[21] Yadav N A, Ohri A and Das N, "Analysis of Thermal Pattern Variation for River Ganges with Satellite Imagery"; Journal of Water Resource Engineering and Management, **7(3),** 21-30, (2020).

[22] Rai P K, Mishra A and Tripathi B D, " Heavy metal and microbial pollution of the River Ganga: A case study of water quality at Varanasi"; Aquatic Ecosystem Health & Management, **13(4),** 352-361, (2010).

[23] Pandey J and Singh R , "Heavy metals in sediments of Ganga River: up-and downstream urban influences"; Applied Water Science, **7(4),** 1669-1678, (2017).

[24] Reuter D C, Richardson C M, Pellerano F A, Irons J R, Allen R G, Anderson M, "The Thermal Infrared Sensor (TIRS) on Landsat 8: Design overview and pre-launch characterization"; Remote Sensing, **7(1),** 1135-1153, (2015).

[25] Kuhn C, de Matos Valerio A, Ward N, Loken L, Sawakuchi H O, Kampel M, "Performance of Landsat-8 and Sentinel-2 surface reflectance products for river remote sensing retrievals of chlorophyll-a and turbidity"; Remote Sensing of Environmemt, **224,** 104-118, (2019).

[26] Pahlevan N, Chittimalli S K, Balasubramanian S V and Vellucci V, "Sentinel-2/Landsat-8 product consistency and implications for monitoring aquatic systems"; Remote Sensing of Enviroment, **220,** 19-29, (2019).

[27] Lacaux J P, Tourre Y M, Vignolles C, Ndione J A and Lafaye M , "Classification of ponds from high-spatial resolution remote sensing: Application to Rift Valley Fever epidemics in Senegal"; Remote Sensing of Environment, **106(1),** 66-74, (2007).

[28] R.N.Simon, T.Tormos, P.A.Danis, "Retrieving water surface temperature from archive LANDSAT thermal infrared data: Application of the mono-channel atmospheric correction algorithm over two freshwater reservoirs." International Journal of Applied Earth Observation and Geoinformation, 30, 247-250, (2014).

[29] Barsi, J.A., Lee, K., Kvaran, G., Markham, B.L. and Pedelty, J.A. ; "The Spectral Response of the Landsat-8 Operational Land Imager", Remote Sensing, 6, 10232-10251, (2014).

[30] Rajeshwari, A. and Mani, N.D. , "Estimation of Land Surface Temperature of Dindigul District Using Landsat 8 Data", International Journal of Research in Engineering and Technology, 3, 2319-1163, (2014).